FISEVIER

Contents lists available at ScienceDirect

Biochemical and Biophysical Research Communications





Inhibition of ERK 1/2 pathway downregulates YAP1/TAZ signaling in human cardiomyocytes exposed to hyperglycemic conditions



Binata Joddar ^{a, b, c, *}, Carla D. Loyola ^{a, b}, Salma P. Ramirez ^{a, b}, Abhinaya Muruganandham ^d, Irtisha Singh ^e

- a Inspired Materials & Stem-Cell Based Tissue Engineering Laboratory (IMSTEL), The University of Texas at El Paso, El Paso, TX, 79968, USA
- ^b Department of Metallurgical, Materials, and Biomedical Engineering, M201 Engineering, The University of Texas at El Paso, 500 W. University Avenue, El Paso, TX, 79968, USA
- ^c Border Biomedical Research Center, The University of Texas at El Paso, 500 W. University Avenue, El Paso, TX, 79968, USA
- ^d Department of Biomedical Engineering, College of Engineering, Texas A&M University, College Station, TX 77843, USA
- ^e Department of Molecular and Cellular Medicine, College of Medicine, Texas A&M University Health Science Center, 8447 Riverside Pkwy Medical Research and Education Building II, Suite 4344, Bryan, TX, 77807-3260, USA

ARTICLE INFO

Article history: Received 28 December 2022 Received in revised form 4 January 2023 Accepted 6 January 2023 Available online 7 January 2023

Keywords:
Cardiomyopathy
Reactive oxygen species (ROS)
Type-II Diabetes
Hyperglycemia
Cardiomyocyte
RNA Sequencing

ABSTRACT

Hyperglycemia-mediated cardiac dysfunction is an acute initiator in the development of vascular complications, leading to cardiac fibrosis. To investigate the effects of hyperglycemia-mediated changes in cardiomyocytes, cells were cultured in-vitro under normoglycemic (5 mM or 25 mM D-glucose) and hyperglycemic (5 → 50 mM or 25 → 50 mM D-glucose) conditions, respectively. After 24-h of hyperglycemic exposure, cells were collected for RNA-sequencing (RNA-seq) studies to further investigate the differentially expressed genes (DEG) related to inflammation and fibrosis in samples cultured under hyperglycemic-in comparison with normoglycemic-conditions. Western Blotting was done to evaluate the protein expression of YAP1/TAZ under hyperglycemia induced stress conditions, as it is known to be involved in fibrotic and vascular inflammatory-mediated conditions, RNA-seq revealed the DEG of multiple targets including matrix metalloproteinases and inflammatory mediators, whose expression was significantly altered in the 5 \rightarrow 50 mM in comparison with the 25 \rightarrow 50 mM condition. Western Blotting showed a significant upregulation of the protein expression of the YAP1/TAZ pathway under these conditions as well (5 \rightarrow 50 mM). To further probe the relationship between the inflammatory extracellular-signal-regulated kinase (ERK 1/2) and its downstream effects on YAP1/TAZ expression we studied the effect of inhibition of the ERK 1/2 signaling cascade in the 5 \rightarrow 50 mM condition. The application of an ERK 1/2 inhibitor inhibited the expression of the YAP1/TAZ protein in the 5 \rightarrow 50 mM condition, and this strategy may be useful in preventing and improving hyperglycemia associated cardiovascular damage and inflammation.

© 2023 Elsevier Inc. All rights reserved.

1. Introduction

In patients with diabetes mellitus, the presence of myocardial dysfunction in the absence of well-known clinical cardiovascular ailments such as a coronary artery or valvular disease, and other conventional risk factors, such as hypertension and dyslipidemia,

E-mail address: bjoddar@utep.edu (B. Joddar).

has led to the overall description and terminology for diabetic cardiomyopathy (DCM). DCM is one of the major complications caused by diabetes mellitus and is often linked to prolonged hyperglycemia in Type-II diabetes [1]. Some studies have suggested that an important consequence of prolonged and pre-existing hyperglycemia is cardiomyocyte apoptosis, which can lead to the loss of contractile cardiac tissue and initiate cardiac remodeling [2,3]. Consequently, the loss of ventricular cardiomyocytes, followed by the hypertrophy of the remaining viable cardiomyocytes and the development of cardiac dysfunction are the typical characteristics of DCM [4]. However, the mechanisms by which hyperglycemia induces myocardial apoptosis and cardiac dysfunction are not

^{*} Corresponding author. Inspired Materials & Stem-Cell Based Tissue Engineering Laboratory (IMSTEL), Department of Metallurgical, Materials, and Biomedical Engineering, M201 Engineering, The University of Texas at El Paso, 500 W. University Avenue, El Paso, TX, 79968, USA.

completely understood.

Hyperglycemia may induce the activation of reactive oxygen species (ROS) through the stimulation of the glycation reaction and electron transport chain in mitochondria in cardiac cells [5]. The initiation of cardiac dysfunction leading to DCM is believed to be associated with the incidence of such ROS species which act as key signaling molecules and play an important role in the progression of inflammatory cardiovascular disorders [6]. An enhanced ROS generation due to inflammation can cause cardiac cell dysfunction and tissue injury via the activation of pro-inflammatory mechanisms [5,6]. In order to identify and isolate some of these selected mechanisms, we developed an in vitro model of Hyperglycemia-Induced Stress on human AC16 cardiomyocytes, in the present study. For doing this, we exposed human AC16 cardiomyocytes to varying doses of hyperglycemic treatments and performed RNA sequencing (RNA-seq) and subsequent analysis. Differentially expressed genes (DEGs) between the varying hyperglycemic conditions were used to understand the effects on a human cardiomyocyte cell model and evaluated. Gene Ontology (GO) enrichment analysis was used to study and identify a selected set of genes that were up-regulated under hyperglycemic conditions, in comparison with control sets.

Prior studies have demonstrated that, in response to stress, the cardiac tissue undergoes alterations in metabolism, ranging from changes in substrate utilization to mitochondrial function, collectively called metabolic remodeling [7]. However, the molecular mechanisms mediating metabolic remodeling in the cardiac tissue remains unclear. Among the key transcriptional factors that play an important role in the regulation of cellular homeostasis of cardiomyocytes, the Yes-associated protein 1 (YAP1) and the transcriptional coactivator with PDZ-binding motif (TAZ) from the Hippo signaling pathway are major downstream effectors [8], involved in both normal and diseased conditions.

So, we performed Western blotting to evaluate the role of YAP1/TAZ in mediating cardiac tissue injury during hyperglycemia-induced stress conditions. We used information generated from the results of RNA-seq, DEG, and GO enrichment analysis to identify pathways that are perturbed by hyperglycemic culture conditions in cardiomyocytes. From these results, we selectively chose to study the effect of the inhibition of the well-known oxidative stress-mediated inflammatory pathway, ERK 1/2 signaling cascade, and its downstream effects on YAP1/TAZ expression. The addition of an ERK 1/2 inhibitor prior to hyperglycemic shock, inhibited the enhanced expression of the YAP1/TAZ proteins in the cardiomyocytes.

Thus our study for the first time highlights the modulatory role of oxidative stress-mediated inflammatory mechanisms in cardiac cell transcriptome dynamics in cultures of cardiomyocytes exposed to high and varying glucose conditions. This work paves the way for establishment of a hyperglycemic human cardiac cell specific model for in-vitro tissue-on-a-chip studies.

2. Experimental procedures

2.1. Cell culture

The human cardiomyocyte (CM) cell line AC16, was purchased from EMD Millipore (Billerica, MA, USA) and maintained in (DMEM; Invitrogen, Carlsbad, CA, USA) containing 10% fetal bovine serum (FBS; Gibco, Carlsbad, CA, USA), 100 U/mL penicillin and 100 mg/mL streptomycin (Invitrogen, MA, USA) and cultured with either 5 mM or 25 mM D-glucose in a humidified incubator at 37°C with 5% CO₂ for at least 3-passages prior to them being used for experiments. Please refer to supplementary section S2.1 for additional details for cell culture.

2.2. Induction of hyperglycemia-induced stress

Cells derived from respective cultures maintained with specific glucose concentrations (section 2.1) were trypsinized, passaged and cultured in 6-well plates with 2×10^5 cells/well supplemented with either 5 mM or 25 mM glucose for 24 h followed by increasing the concentration of glucose supplementation to 50 mM in both sets of cultures (5 \rightarrow 50 and 25 \rightarrow 50) for the next 24 h afterward. Briefly, an additional amount of D-Glucose was added to supplement for the additional 45 mM glucose or the additional 25 mM glucose in the two culture systems in parallel, to represent a hyperglycemic-induced stress condition consisting of 50 mM glucose in total, for 24 h. To measure the incidence of ROS, DHEfluorescent staining was utilized in cells treated with varying hyperglycemic treatments (5 \rightarrow 50 mM and 25 \rightarrow 50 mM respectively). DAPI was utilized to stain the cell's nucleus. DHE stained cells represented cells containing intracellular superoxide in red while the DAPI (4',6-diamidino-2-phenylindole) stain represented the total number of cell nuclei in blue and was quantified using Equation (1):

DHE / DAPI (%) =
$$\frac{\text{\# of red cells}}{\text{Total } \# \text{ of red and blue cells}} x100$$
 (1)

Additionally, a Live-Dead assay was performed to test the cells' viability after the hyperglycemic treatments. Calcein AM represented live cells in green while ethidium homodimer represented dead cells in red. The viability of cells was quantified using **Equation (2)**:

No. of live
$$\sqrt{\text{dead cells }(\%)} = \frac{\# \text{ of green or red cells}}{\text{Total } \# \text{ of green and red cells}} x 100$$
(2)

2.3. RNA isolation

Total RNAs from the AC16CMs cultures were extracted with TRIzol reagent (Invitrogen, Thermo Fisher Scientific, Inc., Wilmington, DE, USA) following the manufacturer's protocol and additional details are presented in supplementary section S2.3.

2.4. RNA-sequencing, DEG's detection and GO-enrichment analysis

RNA-seq data was processed and analyzed as described in Ref. [9]. DEG's identification and GO enrichment analysis were also performed as described in Ref. [9]. Library preparation and deep sequencing were performed according to the manufacturer's protocol (Illumina, Welgene Biotechnology Company, Taipei, Taiwan), following published reports [9] and additional details are presented in supplementary section S2.4.

2.5. Quantitative PCR (qPCR) analysis

To validate the results from RNA sequencing, selected genes were studies using RT-PCR. For this experiment total RNA extraction was carried out using RNeasy® Plus Mini Kit (QIAGEN. Hilden, Germany) according to the manufacturer's instructions. Extracted RNAs were quantified by NanoDrop OneC spectrophotometer (ThermoFisher Scientific, Waltham, MA, USA) and the absorbance ratios at 260/280 nm and 260/230 nm were measured to determine RNA purity and the data is shown below in Table 1.

Please refer to supplementary section S2.5 for additional details on the procedures. The target genes selected for further analysis

Table 1Absorbance ratios at 260/280 nm and 260/230 nm to determine RNA purity.

Sample Cardiomyocytes	ng/μl	260/280	230/260
1 3 3			
control 5 mM Glu	259.1	2.09	2.17
Cells 5 mM-50 mM Glu No.1	52.9	2.13	1.30
Cells 5 mM-50 mM Glu No.2	17.7	2.11	1.29
Cells 5 mM-50 mM Glu No.3	18.5	2.20	0.36
control 25 mM Glu	16.7	2.15	0.15
Cells 25 mM-50 mM Glu No.1	262.4	2.10	2.11
Cells 25 mM-50 mM Glu No.2	216.3	2.10	2.21
Cells 25 mM-50 mM Glu No.3	157.2	2.10	0.61

were TGF β 1, MYOCD, CCL2 and MMP3 while GAPDH was used as reference gene (control). The results helped derive the value of the fold change in expression from the target genes (TGFB1, MYOCD, CCL2 and MMP3) normalized with the reference gene, GAPDH.

2.6. Western blotting

After the exposure of cell cultures to varying hyperglycemic conditions (5 \rightarrow 50 mM and 25 \rightarrow 50 mM) for a total of 24 h, the AC16 cells were harvested using lysis buffer with protease and phosphatase inhibitors and processed for western blotting of YAP1/TAZ as described in our previous work [10] and reported in detail in supplementary section S2.6.

2.7. ERK 1/2 inhibitor studies

AC16 cells cultured using normoglycemic conditions (5 mM) and at 70% confluence in 12-well plates were used for this experiment. From a total of 12 samples, a set of 6 samples of cells in wells was exposed to 500 nM inhibitor of ERK 1/2 (Ulixertinib BVD-523; Selleck Chemicals LLC, Houston. TX) for 4 h [11]. Out of those 6 samples, 3 were further treated using hyperglycemic conditions with 50 mM Glucose for 24 h. Another set of 3 samples was maintained at normoglycemic conditions. For the remaining 6 samples not treated with the inhibitor, 3 samples were cultured using hyperglycemic conditions with 50 mM Glucose for 24 h, and the remaining 3 samples were maintained at normoglycemic conditions. The immunocytochemistry procedure was performed as follows after 24 h in all wells and reported in detail in supplementary section S2.7.

For determining the level of cellular fluorescence associated with the YAP1/TAZ expression in the images acquired ImageJ (NIH) was used [12]. Briefly, the DAPI (blue) images was split and separated from the YAP1/TAZ (green) and the latter set of images were further processed. Next, the cell of interest (ROI) was selected using a freehand tool. From the Analyze menu "set measurements" was selected to obtain intensity values. Three repeated measurements were made from the same cell to obtain mean intensity values. An area next to the fluorescence was selected to serve as the background for this measurement. At least ten different cell measurements were made from one image and for each condition three sets of images were analyzed to report on Mean \pm SD for the YAP1/TAZ protein expression.

2.8. Statistical analysis

Statistical analysis was performed in GraphPad Prism. Plots were graphed as means and SD, and statistical significance is presented as *p < 0.05 (two-tailed) and was considered to indicate a statistically significant difference. The expression levels of the proteins were compared between cells treated with varying hyperglycemic treatments (5 \rightarrow 50 and 25 \rightarrow 50) using ANOVA,

followed by Dunnett's test.

3. Results

3.1. Oxidative stress generation and cytotoxicity

Hyperglycemic shock treatment was initiated by glucose supplementation to 50 mM in both sets of cultures (5 \rightarrow 50 and $25 \rightarrow 50$ mM) for an additional 24 h. The expression of Reactive Oxygen Species (ROS) was measured using Dihydroethidium (DHE) fluorescent staining; and the identification of viable and non-viable cells was performed using a Live/Dead Assay and fluorescent staining, as well. The representative microscopy images obtained after hyperglycemic shock treatment and ROS staining are shown in Fig. 1(A). In addition, quantification of these results is shown in Fig. 1(B). The total number of cells stained with DHE is mostly equivalent to the total number of nuclei stained with DAPI, which confirms the association between the incidence of ROS species related to hyperglycemic exposure. The DHE/DAPI percentage was calculated using Equation (1) and the percentage detected in $5 \rightarrow 50$ mM samples was $49.1\% \pm 1.18$. The percentage of cells stained with DHE/DAPI detected in the 25 \rightarrow 50 mM samples was $49.4\% \pm 1.13$ and these values were not statistically different.

The representative live-dead confocal microscopy images (Fig. 1(A)) are depicted alongside the DHE-DAPI staining results. Likewise, Fig. 1(C) shows a quantification of the results obtained, and as can be observed, there is a greater percentage of live cells in comparison with dead cells, present in both hyperglycemic treatment conditions. Cell viability in both conditions was calculated using **Equation (2)**. A 97% \pm 3.6 cell viability was detected in 5 \rightarrow 50 mM samples whereas, 98.5% \pm 2.5 was detected in the 25 \rightarrow 50 mM samples. Since the hyperglycemic exposure was provided only for 24 h, therefore, it can be concluded that the hyperglycemic treatments did not cause cell death via apoptosis.

3.2. Hyperglycemia changes cardiomyocytes transcriptome

The extracted RNA from the AC16 cardiomyocytes cultures was used to identify the genes that changed expression under different treatments (Fig. 2). Shown in Fig. 2 (A-B) is a heatmap of DEG (row-scaled z-score of log₂FPKM of DEGs, P-adj <0.05) associated with varying hyperglycemic shock treatments. It shows the DEGs between cell samples treated with 25 \rightarrow 50 mM and 5 \rightarrow 50 mM in comparison with their respective controls. Between 5 \rightarrow 50 mM samples we detected higher number of genes with significantly different expression levels (n = 187) in comparison to cells treated with 25 \rightarrow 50 mM condition (n = 50), suggesting that a higher dose of hyperglycemic exposure (5 \rightarrow 50 mM) significantly alters the transcriptome.

As can be observed in Fig. 2(A), the cardiomyocytes treated with a hyperglycemic shock from $25 \rightarrow 50$ mM of glucose, showed an up-regulation in the expression of the following genes in comparison to the control samples (25 mM). This included targets such as Fibronectin 1 (FN1), Transforming Growth Factor Beta-2 (TGFβ-2), Collagen Type IV Alpha 1 (COL4A1), Collagen Type IV Alpha 2 Chain (COL4A2), Tenascin-C (TNC), and Serine Proteinase Inhibitor (SER-PINE 1) all of which can be classified under pathways responsible for extracellular matrix organization and inflammatory response. Additionally, in the cells treated with a hyperglycemic shock from $5 \rightarrow 50$ mM of glucose, as shown in Fig. 2(B), the DEG expression showed a significant change in comparison to both the controls (5 mM) and the 25 \rightarrow 50 mM samples. Genes showing an upregulation in this case included Ephrin Type-A Receptor 2 (EPHA2), Interleukin 6 (IL6), Fibroblast Growth Factor 2 (FGF2), Proto-Oncogene BHLH Transcription Factor (MYC), Platelet-Derived

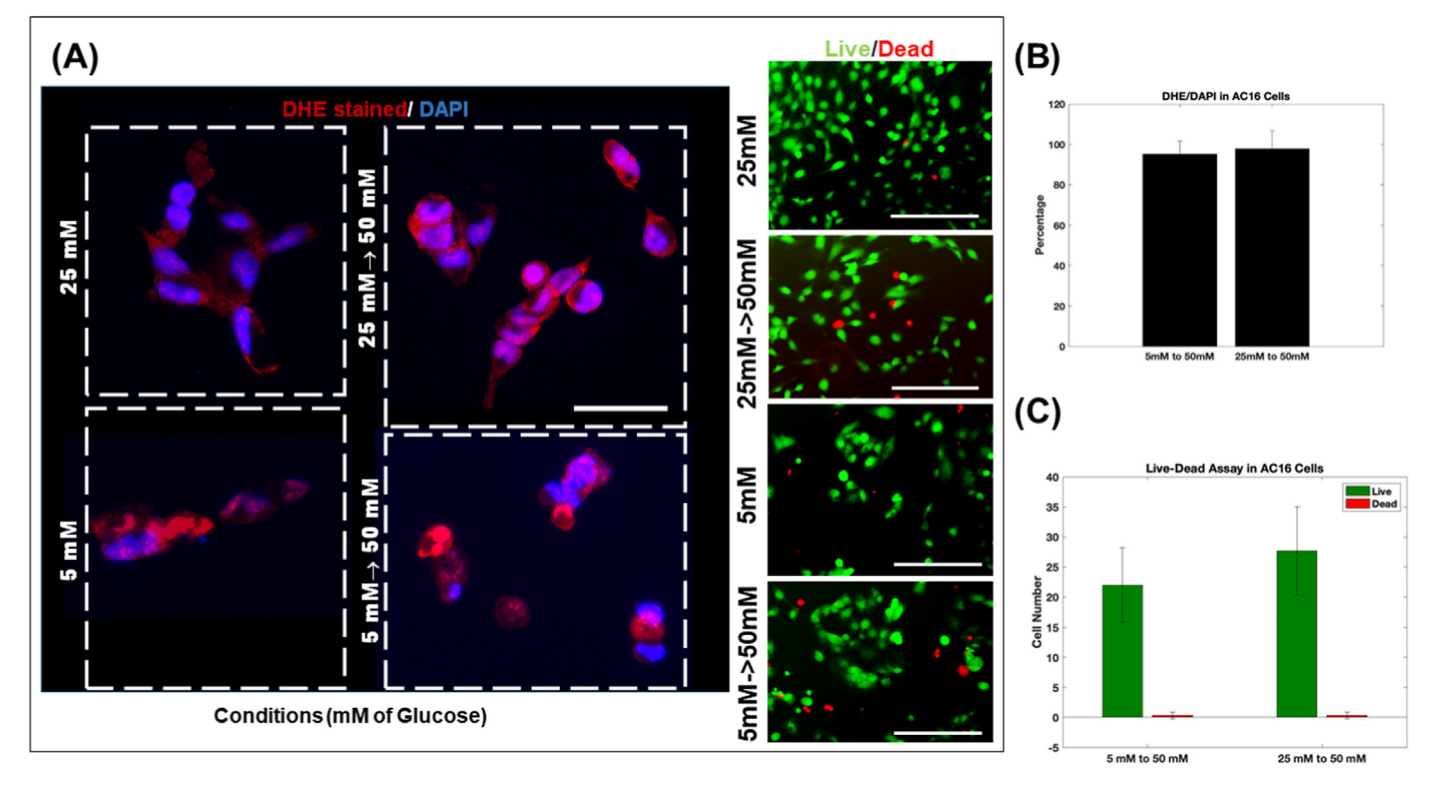


Fig. 1. Reactive Oxygen Species and Live-Dead assay. (A) Dihydroethidium (DHE)-Reactive Oxygen Species (ROS) staining depicts ROS directly in live cells for all cultures depicted. Shown alongside are cell viability results performed using Live-Dead assay. The scale bar depicts 100 μm for all images. (B) Depicts the quantification of DHE stained cells expressed as a percentage of total number of DAPI stained cells in all cultures. (C) Depicts the quantification of Live and Dead cell numbers in all cultures. This data confirms that the glucose shock treatments i.e. 25-50 mM and 5-50 mM did not lead to cell death even though varying expression of ROS was observed in both sets of cultures.

Growth Factor Receptor-Beta (PDGFRB), Transforming Growth Factor Beta-1 (TGF β 1), Transforming Growth Factor Beta-2 (TGF β 2), C-X-C Motif Chemokine Ligand 10 (CXCL10), C-X-C Motif Chemokine Ligand 12 (CXCL12), Matrix Metallopeptidase 3 (MMP3), Collagen Type IV Alpha 1 (COL4A1), Collagen Type III Alpha 1 Chain (COL3A1), Tripartite Motif Containing 22 (TRIM22), C-C Motif Chemokine Ligand 2 (CCL2), Vascular Endothelial Growth Factor C (VEGFC), Myocardin (MYOCD), Hypoxia Inducible Factor 1 Subunit Alpha (HIF1A), Serine Proteinase Inhibitor (SERPINE 1), and Tenascin C (TNC). These targets can be classified under pathways responsible for cellular response to external stress-related stimuli leading to extracellular matrix organization and the regulation of the inflammatory cascade (ERK 1 and 2).

We next performed gene ontology (GO) pathway enrichment analysis of DEGs to identify pathways that are perturbed by the $5 \rightarrow 50$ mM hyperglycemic conditions in comparison with the $25 \rightarrow 50$ mM condition. To do this, we used the Bioconductor package GOstats to perform hypergeometric-based tests and generate significant ontology terms related to biological processes. GO terms related to known biological processes and biochemical pathways associated with vascular inflammation, cellular response to stimulus and extracellular matrix reorganization were identified (P <0.01). A number of DEGs were common between the two treatment groups but the cell cultures treated with the 5 \rightarrow 50 mM hyperglycemic conditions, exhibited a large difference in the number of DEGs, more so than that of $25 \rightarrow 50$ mM. However, the ERK 1/2 and the JAK-STAT cascade signaling which are implicated in cardiovascular disease and inflammation was significantly highlighted in our GO analysis under both sets of experimental hyperglycemic conditions, Fig. 2(C).

From the DEG analysis, the expression of matrix

metalloproteinase-3 (MMP3), and the following inflammatory mediators, Interleukin-6 (IL-6), C-X-C Motif Chemokine Ligand 10 (CXCL10) and C-C Motif Chemokine Ligand 2 (CCL2) were selected to study the changes in gene expression. As can be observed in Fig. 3(A), the DEG for MMP-3 was significantly affected in the $5 \rightarrow 50$ mM hyperglycemic condition in comparison with 5 mM, on the other hand, it can be observed that the $25 \rightarrow 50$ mM samples did not show a significant difference in comparison to the control (25 mM) samples. This trend was also observed for IL-6, CXCL10, and CCL2 gene expression, in which the higher change in DEG levels is shown in the $5 \rightarrow 50$ mM hyperglycemic condition, as can be observed in Fig. 3(B), 3(C), and 3(D) respectively. Data in Fig. 3 includes results from at least 2 replicates in each condition reported. These results further confirmed the significant perturbation of pathways responsive to hyperglycemic stress-related stimuli leading to extracellular matrix organization and the regulation of the inflammatory cascades in the samples treated with $5 \rightarrow 50$ mM hyperglycemic conditions.

3.3. Selective validation of RNA-sequencing outcomes

For the qPCR analysis we selected a sub-group of genes, the CCL2 and the MMP3 gene to confirm the data obtained in the large-scale RNA-seq. studies to further confirm their varying expression in samples treated with a glucose shock of $5 \rightarrow 50$ mM of glucose, in comparison with normoglycemic controls (5 mM). As can be observed in Fig. 3(E), the relative expression of CCL2 in comparison with GAPDH was significantly up regulated in comparison to the control samples. A similar result was observed for MMP3 which was up-regulated as well in comparison to the controls. These results confirmed and validated the trends in DEG that were reported

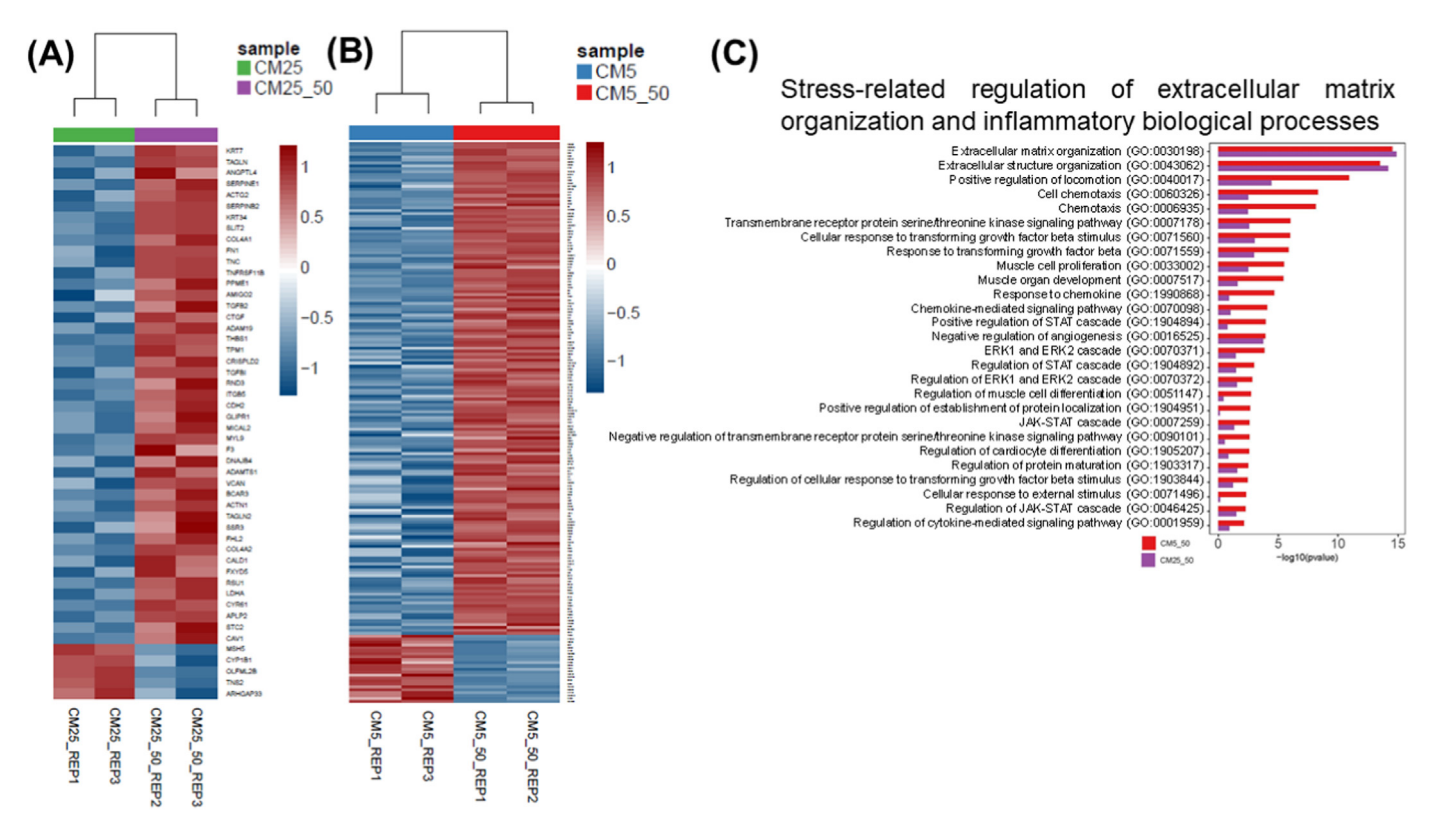


Fig. 2. RNA sequencing and GO analysis. Heatmap expression of differentially expressed genes in 25-50 mM (A, n=50) and 5-50 mM (B, n=187) in comparison with their respective (25 mM and 5 mM) controls (row-scaled z-score of log_2FPKM of DEGs, P-adj <0.05). Overall gene expression was significantly perturbed in the 5-50 mM culture condition (versus 5 mM) in comparison to the 25-50 mM condition (versus the 25 mM). Therefore this data it suggests that the 5-50 mM condition poses a significant hyperglycemic shock treatment for these cells in the culture conditions reported, in this study. (C) GO enrichment analysis in the 5-50 mM and 25-50 mM glucose conditions showed perturbation of pathways responsible for cellular response to external stress-related stimuli leading to extracellular matrix organization and the regulation of related inflammatory cascades in both sets of hyperglycemic shock treatments (P < 0.01). (For interpretation of the references to colour in this figure legend, the reader is referred to the Web version of this article.)

in this study using RNA-seq. analysis.

3.4. Hyperglycemia alters the protein expression of YAP1/TAZ

Western blot analysis manifested that the expression of YAP1/ TAZ was altered significantly under the 5 \rightarrow 50 mM hyperglycemic treatment as observed in Fig. 4(A-B) (p < 0.02). Additionally, the $5 \rightarrow 50$ mM samples showed a greater difference in YAP protein expression when compared to control samples (5 mM). Moreover, these results showed an upregulation of the YAP1/TAZ protein expression in cells treated with a hyperglycemic treatment of $5 \rightarrow 50$ mM in comparison to the cells treated with a hyperglycemic treatment of 25 \rightarrow 50 mM (Fig. 4(A)). In contrast, the $25 \rightarrow 50$ mM samples showed an expression similar to the controls (25 mM: Fig. 4(A)) however, it can be observed that the TAZ expression was up-regulated in the 25 \rightarrow 50 mM samples. Additionally, the $5 \rightarrow 50$ mM condition shows an up-regulation for both YAP1 and TAZ respectively when compared to the 5 mM condition. These results confirm that the $5 \rightarrow 50$ mM condition posed as a significant modulator for the alteration of cellular biochemical pathways to selectively enhance the protein expression of YAP1/ TAZ, in this study.

3.5. Effects of inhibition of ERK-1/2 on YAP1/TAZ expression in the presence of hyperglycemic conditions

GO enrichment analysis (Fig. 2(C) and Supplementary Fig. 1) shows perturbation of pathways responsible for cellular response

to external stress-related stimuli leading to extracellular matrix organization and the regulation of related inflammatory cascades in both sets of hyperglycemic shock treatments. The 5 \rightarrow 50 mM condition upregulated more targets compared to the 25 \rightarrow 50 mM condition. Thus, the 5 \rightarrow 50 mM hyperglycemic condition was selected further to study the effect of ERK 1/2 inhibition on downstream signaling pathways in this study.

To validate the effect on the ERK 1/2 signaling pathway, we treated cells cultured using $5 \rightarrow 50$ mM hyperglycemic conditions for 24 h in the presence and absence of a pharmacological ERK 1/2 inhibitor. Immunofluorescence staining was performed to evaluate the effect of ERK 1/2 inhibition on the YAP1/TAZ protein expression (Fig. 5).

Specifically, our results showed an enhanced expression of the YAP1/TAZ pathway in hyperglycemic cardiomyocyte cultures (5 \rightarrow 50 mM) Fig. 5(B) in comparison with control conditions (5 mM), Fig. 5(A). This effect was reversed when the ERK 1/2 inhibitor was added to the cultures prior to them being exposed to hyperglycemic cardiomyocytes (5 \rightarrow 50 mM), Fig. 5(D). The inhibitor by itself did not pose any cytotoxicity as shown in Fig. 5(C). Quantitative expression of YAP-1/TAZ expression is shown in Fig. 5(E), in which the 5 \rightarrow 50 mM condition showed a significant enhancement (p < 0.02) of the YAP/TAZ protein expression in comparison with all other conditions. Our results strongly indicate that the ERK 1/2 signaling cascade may be involved in regulating the expression of YAP1/TAZ mechanism in cells treated using 5 \rightarrow 50 mM hyperglycemic conditions.

This study confirmed that the ERK 1/2 pathway has a

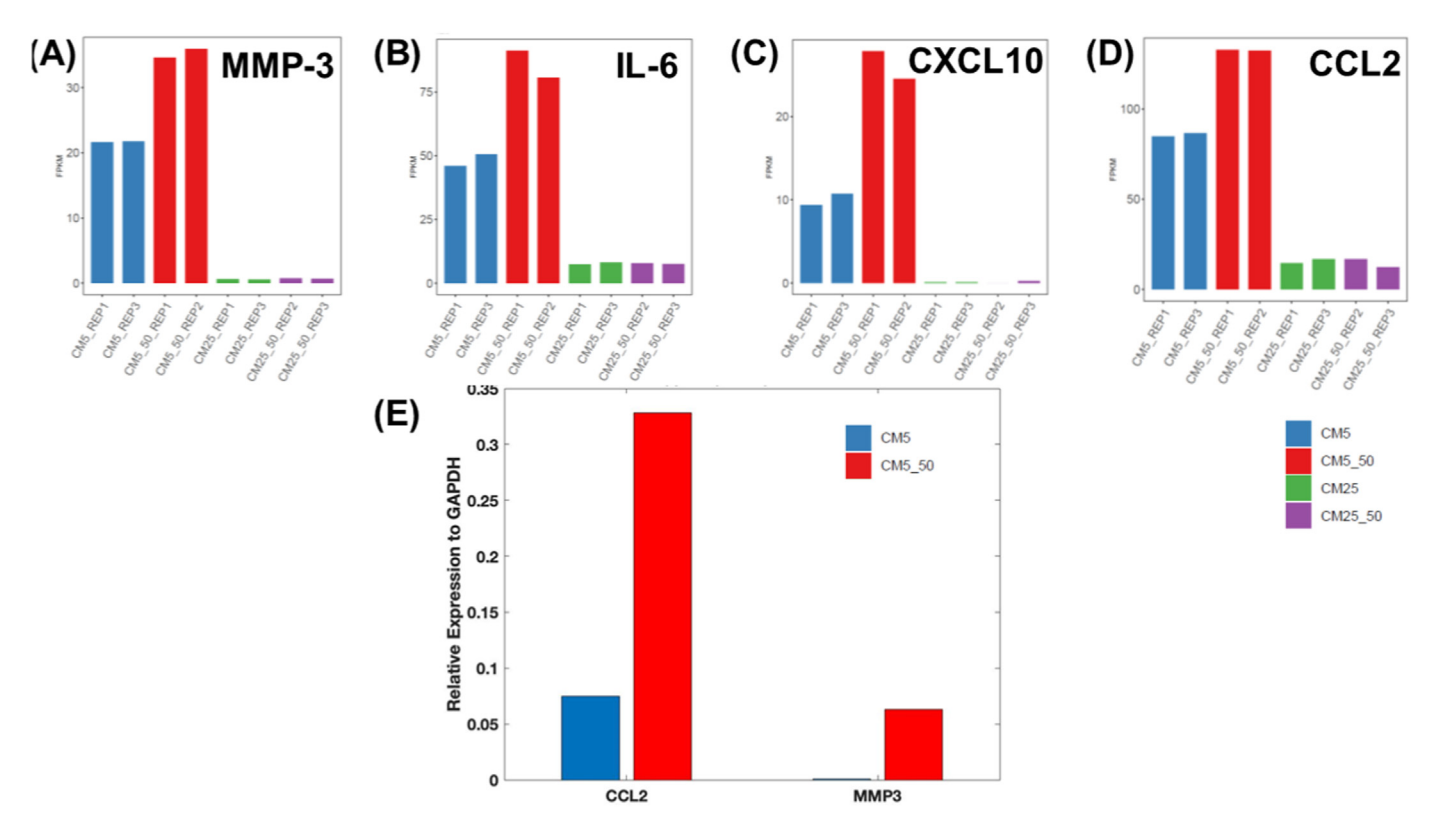


Fig. 3. Differential expression gene (DEG) analysis (A—D) to discover quantitative changes in expression levels of selected genes including MMP-3, IL-6, CXCL10, and CCL2 between experimental groups. RNA-seq studies revealed significantly DEGs in the hyperglycemic condition ($5 \rightarrow 50 \text{ mM}$) in comparison with the normoglycemic (5 mM) condition. Among the extracellular matrix proteins, MMP3 (A) was significantly perturbed (shown in FPKM - Fragments per kilo base of transcript per million mapped fragments). Altered expression of inflammatory mediators included the following genes, IL-6 (B), CXCL10 (C), and CCL2 (D). Shown in E is the Quantitative PCR (qPCR) analysis. CCL2 and MMP3 gene expression was selectively studied in cultures treated with 5-50 mM glucose (hyperglycemic) compared with controls (5 mM) and the data was normalized to GAPDH expression in both conditions (7 mm), and the data was normalized to GAPDH expression in both conditions (7 mm). The expression of both genes was significantly up-regulated in the 7 mm compared to controls. These results confirmed the trends shown by our RNA-seq data and validated DEG results obtained in this study.

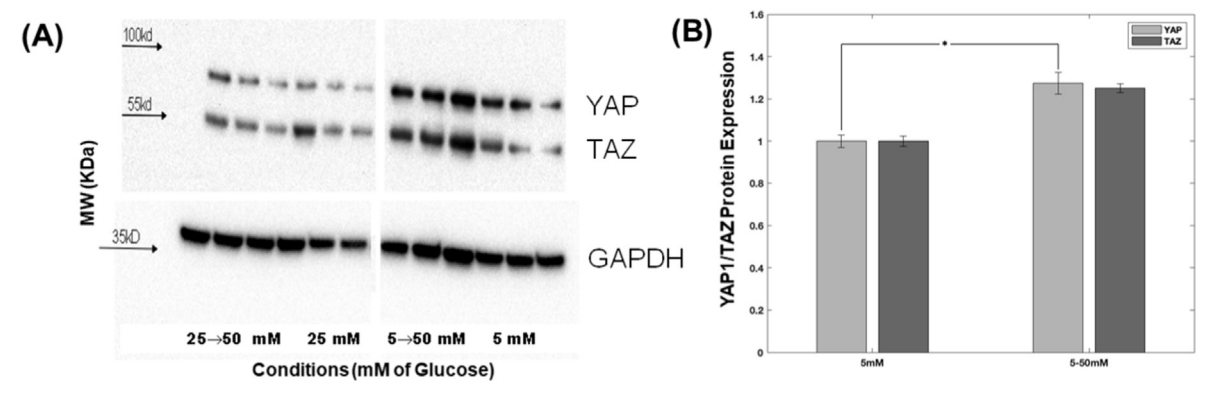


Fig. 4. Western Blotting Analysis. Results showed a significant upregulation of the protein expression of the YAP1/TAZ pathway in hyperglycemic cardiomyocytes (5–50 mM) in comparison with other conditions in (A) and (B).

modulatory effect on the Hippo/YAP pathway in human AC16 cardiomyocytes. The inhibition of ERK 1/2 by a specific inhibitor decreased the YAP1 expression in the cells, which suggests that the YAP1/TAZ mechanism can be correlated with the ERK 1/2 EGFR-RAS-MAPK signaling in human cardiac physiology [13,14].

4. Discussion

Diabetes mellitus is a major risk factor for the development of cardiovascular disease and oxidative stress plays an important role in this process. From prior published studies by others it has been implied that higher glucose levels increase generation of mitochondrial ROS formation [15]. Fluctuating and high glucose levels over a prolonged period can result in oxidative stress, leading to inflammation and altered epigenetic mechanisms [16]. Therefore, we investigated the effects of hyperglycemia on the formation of ROS on cardiomyocytes. Although both $5 \rightarrow 50$ mM and $25 \rightarrow 50$ mM hyperglycemic-stress concentrations may be used as models for cardiac hyperglycemia, the concentration of $5 \rightarrow 50$ mM was found to be more ideal for simulating cardiac hyperglycemic

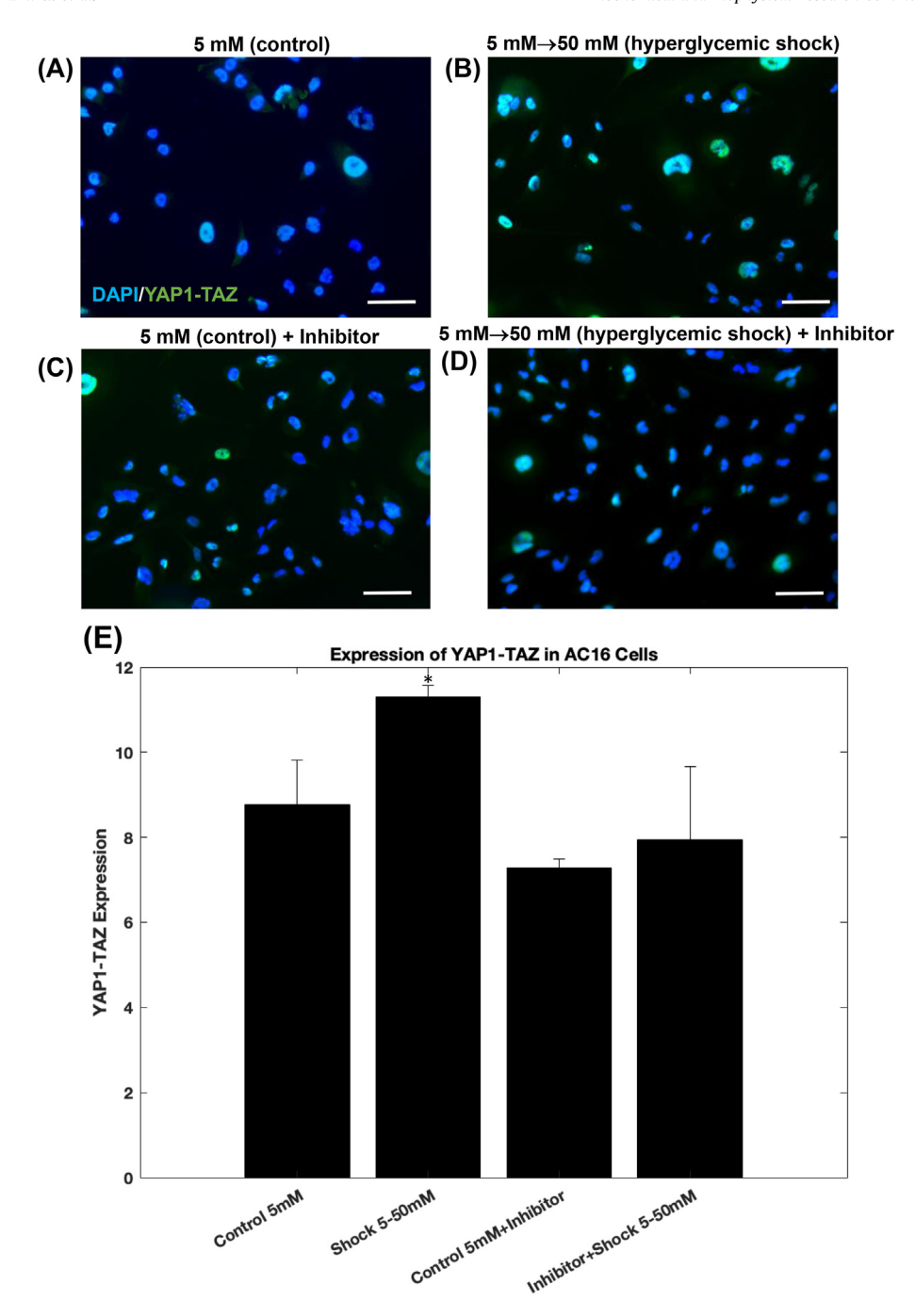


Fig. 5. *ERK 1/2 inhibition on YAP1/TAZ expression.* (A—D) Immunofluorescence results showed a significant expression of the YAP1/TAZ pathway in hyperglycemic cardiomyocytes (5–50 mM) (B) in comparison with control conditions in (A). This effect was reversed when the inhibitor was added to the cultures treated with hyperglycemic cardiomyocytes (5–50 mM) (D). The inhibitor by itself did not adversely affect the cells as shown in (C). Scale bar corresponds to 100 μm in all images. Shown in (E) is a numerical analysis of the YAP1/TAZ intensity in images (A—D) plotted for comparison.

conditions due to significant stress generation as shown by this study. Since the exposure was only provided to these cultures for a total of 24 h, this may have avoided glucose starvation-induced oxidative stress and cell death.

The genes that were differentially expressed in the $25 \rightarrow 50$ mM versus the 25 mM condition included FN1, TGF β 2, COL4A1, COL4A2, TNC, SERPINE1 which were mostly highlighted from our analysis. The DEG of all these candidate genes can be predominantly correlated to altered extracellular matrix organization and cellmatrix adhesion [17]. On the contrary, the genes that were

differentially expressed in the 5 \rightarrow 50 mM versus the 5 mM condition included IL6, FGF2, MYC, PDGFRB, TGF β 1 and TGF β 2, CXCL10, CXCL12, MMP3, COL4A1, COL3A1, TRIM22, CCL2, VEGFC, MYOCD, HIF1A, SERPINE1, TNC which were eminent from our analysis. During the progression of DCM, the factors including CXCL10, CXCL12 and CCl2 are involved in the modulation of cellular responses to stress induced phenomenon such as hyperglycemia. These genes might interplay and execute significant roles via regulation of the glycolysis process. In conclusion, four potential biomarkers including MMP-3, IL-6, CXCL10 an CCL2 were used for

confirmation and validation of DCM prognosis in our model. Published studies have shown that MMP-3 is a significant independent predictor of cardiac events in patients with DCM which was also revealed by our study [18]. With regards to IL6, elevated levels lead to chronic inflammation and fibrotic disorders in cardiac tissues [19]. Prior myocardial infarction studies have shown that long term IL6 signaling, or its over-production plays a causal role in cardiovascular disease [19]. The chemokine CXCL10 is also elevated in cardiovascular diseases, along with an increased infiltration of proinflammatory Th1 and cytotoxic T cells [20]. Thus, CXCL10 is a chemoattractant for these T cells and a polarizing factor for a proinflammatory cardiac phenotype [20]. So, targeting the CXCL10 receptor CXCR3 is a promising therapeutic approach to treating cardiac inflammation [20]. Since our model only consisted of human AC16 CM, it is hard to predict the effect of the altered gene expression of the CXCL10 chemokine receptor in its current state. In future studies, we will include other cell types such as immune cells and macrophages to study the pro-inflammatory phenotype induced by hyperglycemic exposure to cardiomyocytes in an acute and chronic state. The CCL2-CCR2 pathway is recognized as an important physiological modulator and a viable therapeutic target, given its critical role in the immune inflammatory response and a great deal of existing preclinical data that supports the role and involvement of the CCL2-CCR2 axis in experimental cardiovascular disease [21].

Next, our study results suggest that the expression of the YAP1/ TAZ protein, components of the Hippo signaling pathway were significantly was activated and enhanced in the $5 \rightarrow 50$ mM versus the 5 mM samples. This finding correlates with results from other studies where these downstream targets were transcriptionally elevated in the diseased and dysfunctional human and mouse hearts [22]. Interestingly, from such studies adult human hearts had more TAZ than YAP1 as confirmed by their enhanced mRNA and protein expression in diseased hearts although their ratio did not differ much. Our results confirm that YAP1/TAZ signaling is activated in human cardiomyocytes exposed to acute hyperglycemic shock that may eventually lead to cardiac dysfunction. Further investigation with relevant cardiac tissue models will determine whether this pathway is a potential target for preventing and reversing abnormal remodeling during the progression of different cardiac disorders.

It is known that ERK 1/2 signaling mediates a series of molecular alterations and has complex crosstalk with other signaling pathways. The effects of ERK 1/2 inhibition are associated with the Hippo pathway activity. ERK1 and ERK2 have an effect on the Hippo/YAP pathway in human cardiomyocytes such that its dysregulation leads to various congenital cardiac abnormalities [23]. Hippo signaling components are also expressed in the cells of all three cardiac layers (myocardium, epicardium, and endocardium), and play an important role during cardiac development [24]. Since these cells play an important role in cardiac repair and recovery, further research is necessary to better understand how the Hippo/YAP1 signaling pathway regulates them in developing therapeutic interventions without potential adverse effects [24].

Others have proposed that higher glucose levels increase the generation of mitochondrial reactive oxygen species (ROS) resulting in activation of the non-oxidative glucose pathways with hyperglycemia in cardiomyocytes [15]. Subsequently, glycolytic intermediates accumulate and are diverted into the various non-oxidative glucose pathways as indicated. This can lead to activation of mechanisms referred to as 'cardiometabolic complications' which can have detrimental, downstream effects on the heart. Our study for the first time highlighted the role and involvement of

such downstream targets that may be involved in cardio metabolic disorders.

Funding and additional information

Supported by the National Institutes of Health, NIH 1SC1HL154511-01 and the National Science Foundation, NSF 1927628 grants to BJ and NIH 1R21NS121945 to IS.

Data and materials availability

RNA-seq data reported here have been deposited in the Gene Expression Omnibus (GEO) database (accession no. GSE223586; www.ncbi.nlm.nih.gov/geo).

Declaration of competing interest

The authors declare that they have no conflicts of interest.

Acknowledgments

The authors would like to acknowledge the efforts of Dr. Naveen Nagiah, a former postdoc in the Joddar lab for initiating this study. We also acknowledge the efforts of Dr. Munmun Chattopadhayay and Mr. Vikram Thakur at Texas Tech University Health Sciences Center-El Paso for a pilot run of the Western blots.

Appendix A. Supplementary data

Supplementary data to this article can be found online at https://doi.org/10.1016/j.bbrc.2023.01.014.

References

- [1] G. Jia, M.A. Hill, J.R. Sowers, Diabetic cardiomyopathy, Circ. Res. 122 (4) (2018) 624–638.
- [2] A.M. Al Hroob, et al., Pathophysiological mechanisms of diabetic cardiomyopathy and the therapeutic potential of epigallocatechin-3-gallate, Biomed. Pharmacother. 109 (2019) 2155–2172.
- [3] G. Borghetti, et al., Diabetic cardiomyopathy: current and future therapies. Beyond glycemic control, Front. Physiol. 9 (2018) 1514.
- [4] E. Shen, et al., Rac1 is required for cardiomyocyte apoptosis during hyperglycemia, Diabetes 58 (10) (2009) 2386–2395.
- [5] N. Kaludercic, F. Di Lisa, Mitochondrial ROS formation in the pathogenesis of diabetic cardiomyopathy, Front Cardiovasc Med 7 (2020) 12.
- [6] R. Ni, et al., Therapeutic inhibition of mitochondrial reactive oxygen species with mito-TEMPO reduces diabetic cardiomyopathy, Free Radic. Biol. Med. 90 (2016) 12–23.
- [7] T. Doenst, T.D. Nguyen, E.D. Abel, Cardiac metabolism in heart failure: implications beyond ATP production, Circ. Res. 113 (6) (2013) 709–724.
- [8] T. Kashihara, J. Sadoshima, Role of YAP/TAZ in energy metabolism in the heart, J. Cardiovasc. Pharmacol. 74 (6) (2019) 483–490.
- [9] A.M. Brokesh, et al., Dissociation of nanosilicates induces downstream endochondral differentiation gene expression program, Sci. Adv. 8 (17) (2022), eabl9404.
- [10] R. El Khoury, et al., 3D bioprinted spheroidal droplets for engineering the heterocellular coupling between cardiomyocytes and cardiac fibroblasts, Cyborg and Bionic Systems 2021 (2021), 9864212.
- [11] M. Shin, C.E. Franks, K.L. Hsu, Isoform-selective activity-based profiling of ERK signaling, Chem. Sci. 9 (9) (2018) 2419–2431.
- [12] C.A. Schneider, W.S. Rasband, K.W. Eliceiri, NIH Image to Image]: 25 years of image analysis, Nat. Methods 9 (7) (2012) 671–675.
- [13] B.V. Reddy, K.D. Irvine, Regulation of Hippo signaling by EGFR-MAPK signaling through Ajuba family proteins, Dev. Cell 24 (5) (2013) 459–471.
- [14] S. Akhtar, et al., Activation of EGFR/ERBB2 via pathways involving ERK1/2, P38 MAPK, AKT and FOXO enhances recovery of diabetic hearts from ischemiareperfusion injury, PLoS One 7 (6) (2012), e39066.
- [15] R.F. Mapanga, M.F. Essop, Damaging effects of hyperglycemia on cardiovascular function: spotlight on glucose metabolic pathways, Am. J. Physiol. Heart Circ. Physiol. 310 (2) (2016) H153–H173.
- [16] V. Thakur, et al., Changes in stress-mediated markers in a human cardiomyocyte cell line under hyperglycemia, Int. J. Mol. Sci. 22 (19) (2021).
- [17] H. Li, et al., Identification of biomarkers and mechanisms of diabetic

- cardiomyopathy using microarray data, Cardiol. J. 27 (6) (2020) 807-816. [18] T. Ohtsuka, et al., Serum matrix metalloproteinase-3 as a novel marker for risk
- stratification of patients with nonischemic dilated cardiomyopathy, J. Card. Fail. 13 (9) (2007) 752-758.
- [19] J.A. Fontes, N.R. Rose, D. Čiháková, The varying faces of IL-6: from cardiac protection to cardiac failure, Cytokine 74 (1) (2015) 62–68.
- [20] R. Altara, et al., The CXCL10/CXCR3 Axis and cardiac inflammation: implications for immunotherapy to treat infectious and noninfectious diseases of the heart, J Immunol Res 2016 (2016), 4396368.
- [21] H. Zhang, et al., Role of the CCL2-CCR2 axis in cardiovascular disease: pathogenesis and clinical implications, Front. Immunol. 13 (2022), 975367.

 N. Hou, et al., Activation of Yap1/Taz signaling in ischemic heart disease and
- dilated cardiomyopathy, Exp. Mol. Pathol. 103 (3) (2017) 267–275.
- [23] B. You, et al., Inhibition of ERK1/2 down-regulates the Hippo/YAP signaling pathway in human NSCLC cells, Oncotarget 6 (6) (2015) 4357–4368.
- [24] M.M. Mia, M.K. Singh, The Hippo signaling pathway in cardiac development and diseases, Front. Cell Dev. Biol. 7 (2019) 211.